Climate driven trends in tree biomass increment show asynchronous dependence on tree-ring width and wood density variation

Astrid Vannoppen[a,*], Pascal Boeckx[b], Tom De Mil[d], Vincent Kint[a], Quentin Ponette[c], Jan Van den Bulcke[d], Kris Verheyen[e], Bart Muys[a,*]

[a] Division Forest, Nature and Landscape, Department of Earth and Environmental Sciences, University of Leuven, Celestijnenlaan 200E, Box 2411, BE-3001 Leuven, Belgium
[b] Isotope Bioscience Laboratory, Ghent University, Coupure Links 653, BE-9000 Gent, Belgium
[c] Earth and Life Institute, Université Catholique de Louvain, Croix du Sud 2, L7.05.09, BE-1348 Louvain-la-Neuve, Belgium
[d] UGCT-Woodlab-UGent, Ghent University, Laboratory of Wood Technology, Department of Forest and Water Management, Coupure Links 653, BE-9000 Gent, Belgium
[e] Forest & Nature Lab, Ghent University, Geraardsbergsesteenweg 267, BE-9090 Melle-Gontrode, Belgium

ARTICLE INFO

ABSTRACT

Tree growth is a key ecosystem function supporting climate change mitigation strategies. However climate change may induce feedbacks on radial growth and wood density, affecting the carbon sequestration capacity of forests. Using a mixed modeling technique long-term trends in radial growth, wood density and above-ground biomass, defined as the product of the annual basal area growth with the wood density, of common beech (*Fagus sylvatica*) and sessile oak *(Quercus petraea)* in the Belgian Ardennes, were determined and explained using climate drivers of change. This modeling strategy allowed us to determine if the same conclusions can be drawn when only BAI is considered, as is assumed in most carbon sequestration studies, when looking at long-term trends in carbon sequestration. The models indicate that above-ground biomass increment changes over time are more driven by changes in radial growth than by changes in wood density. Nevertheless, the assumption of constant wood density in most carbon sequestration studies is incorrect. Ignoring wood density results in an underestimation of long-term trends in above-ground biomass increment for beech, and an overestimation of above-ground biomass increment for oak. Interesting is that radial growth is mostly driven by climate variables of the current year, whereas wood density is more driven by the climate variables of the previous year. Beech radial growth and wood density is found to be negatively influenced by drought and positively by water availability. Oak radial growth and wood density is negatively affected by late frost and positively by water availability. The findings of this study suggest that radial growth in combination with wood density should be used in carbon sequestration studies as different climate driven long-term trends in radial growth and wood density are found.

1. Introduction

Forests play an important role in the carbon cycle, with an estimated global net annual sink of 2.41 ± 0.42 Pg C (for 1990–2007), 42% of which is allocated to living biomass (Pan et al., 2011). Forest conservation and restoration are therefore considered important mitigation strategies to reduce the greenhouse effect (Grassi et al., 2017). However, the carbon sequestration service delivered by forests may vary over time, in space and among tree species (Luyssaert et al., 2010; Babst et al., 2013). Also, changes in external drivers including climate, carbon dioxide (CO_2) concentration, atmospheric pollutant deposition and forest management influence the forest carbon sink (Ciais et al.,

2005; Pan et al., 2011). Considering the role of forests in the global carbon cycle and their projected part in the implementation of the Paris Agreement (Grassi et al., 2017), it is crucial to further refine our knowledge on the interactions between the changing climate, CO_2 concentration, pollutant deposition and the carbon storing capacity of forests and trees (Fahey et al., 2010).

The most dynamic carbon pool in forests is the standing biomass (Fahey et al., 2010). Understanding which environmental drivers are influencing wood formation in a specific tree species and geographical context is of key importance. Basal area increment (BAI, cm^2) derived from tree-ring width (TRW) data can give a retrospective insight in the climate radial growth relationship. However, to obtain a retrospective

Table 1
Location and characterization of the four forest sites where trees were cored.

Site	Coordinates	Elevation (m.a.s.l.)	Slope (°)	Aspect	Beech trees	Oak trees
Marche-en-Famenne	50°27′N 5°6′E	400	5	South-east	5	10
Libin	50°6′N 5°1′E	360	5	North	13	11
Nassogne	50°6′N 5°3′E	260–300	0	–	17	14
Couvin	50°2′N 4°44′E	300	5	East	7	9

view on above-ground biomass accumulation trends, wood density data are needed as well, but are seldom measured. A recently developed method by Van den Bulcke et al. (2014) allows reliable and cost-effective wood density measurements with an annual resolution using X-ray images of tree cores. The combination of BAI data with wood density measured at an annual scale, gives a long-term retrospective view on above-ground biomass storage and its variability. In most carbon sequestration studies, within-tree wood density is assumed to be constant over time (Bouriaud et al., 2004), but the impact this assumption has on local and national forest carbon assessments remains unclear (Babst et al., 2014; Bouriaud et al., 2015).

Tree radial growth has been changing in European forests over the last decades. Climate change (e.g. increased temperature), increased CO_2 and ozone concentration, and increased nitrogen deposition have been identified as drivers of these growth changes (Bontemps and Esper, 2011; Kint et al., 2012; Babst et al., 2013; Reyer et al., 2013). Besides, wood density might also vary at the same time as radial growth and hence influence the net carbon sequestrated at the tree level. Currently, there is not much knowledge concerning possible long-term trends in wood density (Bontemps et al., 2013). Small density decreases (−2%) have been reported in sessile oak by Bergès et al. (2000) for the period 1811–1993. For common beech a slight centennial decrease (−7.5%, for the period 1900–2000) in wood density was observed by Bontemps et al. (2013). It has been demonstrated that environmental conditions at different times of the year are driving both radial growth and wood density (Briffa et al., 2002; Frank and Esper, 2005; Babst et al., 2014; Björklund et al., 2017). Hence, a faster radial growth could possibly coincide with lower tree ring density, leading together to a neutral effect on carbon sequestration.

In ring-porous tree species, there is a clear distinction between earlywood and latewood. In diffuse porous tree species, there is a gradual change from larger vessels at the beginning of the growing season to smaller vessels at the end of the growing season. Higher growth in ring-porous tree species is expected to result in rings with a higher proportion of latewood (i.e. positive relationship between TRW and wood density) (Bergès et al., 2000). For diffuse porous tree species, the relationship between TRW and wood density is either slightly positive or absent (Bontemps et al., 2013; Babst et al., 2014; Zeller et al., 2017). For conifers there is a quite good understanding of the drivers of wood density (Björklund et al., 2017), for diffuse porous and ring-porous tree species (as beech and oak) this knowledge is much poorer.

BAI and wood density data measured on common beech (diffuse-porous) and sessile oak (ring-porous) cores will be used to study long-term trends in radial growth, wood density and above-ground biomass. Above-ground biomass increment is approximated as the product of BAI and wood density. By applying a multilevel mixed modeling strategy, changes in BAI (further referred to as radial growth), wood density and above-ground biomass increment of individual trees related to tree aging can be separated from possible long-term trends related to calendar year for all trees. First, possible long-term trends in radial growth, wood density and above-ground biomass of common beech and sessile oak are modelled. The detected long-term trends in radial growth, wood density and above-ground biomass are compared in order to determine possible consequences of long-term trends in radial growth and wood density for above-ground biomass increment. In this way we can assess what the consequences are of ignoring wood density (i.e. considering radial

growth as a proxy for carbon sequestration) in carbon sequestration studies. In a next step, the climatic variables influencing radial growth, wood density and above-ground biomass increment are identified in order to get insight in the drivers of the detected long-term changes. In this way we are able to assess the consequences of climate change on radial growth, wood density and aboveground biomass.

2. Material and methods

2.1. Sampling design

For this study 42 common beech (*Fagus sylvatica*) and 44 sessile oak trees (*Quercus petraea*) were selected in four different broadleaved forest sites located in the Belgian Ardennes (Table 1). Confounding environmental factors were reduced to a minimum by selecting trees growing in stands with similar soil conditions, slope and elevation. Selected trees were located on well-drained brown acidic soil (WRB: Dystric Cambisol). Elevation ranged from 260 to 400 m above sea level (m.a.s.l.) and slope from 0 to 5°. Selected trees were (co-)dominant, growing in even-aged stands, and covered a wide range of developmental stages (Table 2 for DBH range and Fig. S1).

2.2. Data collection

2.2.1. Wood density and tree-ring width data

Two cores, taken at 180° (North-South direction), per tree were collected in the winter of 2014 with a 5 mm increment corer (Suunto) at 1 m above ground. After drying the tree cores in paper straws (24 h at 103 ± 1 °C), they were scanned at a resolution of 110 μm with the X-ray CT scanner (NanoWood CT facility, Ghent University). X-ray CT derived tree-ring data has been demonstrated to be sufficient to detect long-term trends (Vannoppen et al., 2017). In order to extract wood density data at an annual resolution, tree-ring boundaries were indicated with the X-ray CT toolchain (De Mil et al., 2016). Afterwards, TRWs were measured on cores, whose surface was cut with a microtome and sanded, with a LINTAB 6 table at a resolution of 10 μm. Crossdating was performed on both wood density and TRW data with COFECHA in combination with Tsap-Win in order to ensure correctly dated series (Holmes, 1983; Grissino-Mayer, 2001; Rinn, 2003).

2.2.2. Forest structural and site quality data

Forest structure and site quality was characterized by measuring additional variables in circular plots (18 m radius) established around

Table 2
General statistics summarized for TRW and wood density for beech and oak. Statistics are calculated on the dataset after removal of juvenile growth (first 30 measured rings of each tree) and starting from this year where data from at least 10 trees are available. sd: standard deviation.

Variable	Beech	Oak
Number of trees	42	44
DBH range (cm) in 2014	31.0–82.5	27.5–87.5
Correlation wood density and Dp	−0.32 ($p < 0.001$)	−0.31 ($p < 0.001$)
Number of rings	2241	2937
Mean ± sd TRW (mm)	2.663 ± 1.278	1.771 ± 0.741
Mean ± sd wood density (kg/m³)	686 ± 49	642 ± 72

every cored trees. FieldMap equipment and software (http://www.fieldmap.cz) was used to measure dendrometrical variables in the winter of 2014. Derived forest structural variables were: crown projection area of the cored tree (CPA, m²), height of the cored tree (H, m), total CPA of trees with diameter at breast height (DBH) > 15 cm in the plot (TotCPA, m²), total basal area of trees with DBH > 15 cm in the plot (TotBA, m²), basal area of trees larger than the cored tree (BAL, m²) and the ratio between the diameter of the cored tree and the average diameter of trees with DBH > 15 cm in the plot (ddg). CPA was determined by mapping the crown edge in the four cardinal directions. In each plot, a soil sample of the mineral soil was taken (depth range from 10 to 15 cm) in the South-East direction relative to the cored tree. pH (5:25 soil:solution, 0.01 M CaCl₂), organic C (OC, %) and N content (dry combustion method), derived C/N ratio, bulk density (g/cm³) and texture (fraction clay, loam and sand in %) were measured on the soil sample to characterize the site quality in each plot.

2.2.3. Meteorological and other emission data

Daily data from the three nearest meteorological stations to each of the four sites were used (Royal Meteorological Institute of Belgium, RMI) to interpolate (using inverse-distance weighting) the climatic data to each forest site for the period 1952 to 2014. Variables were rescaled from daily to (i) monthly, (ii) seasonal and (iii) yearly variables. Considered seasonal variables were: January to March (JFM), April to August (AMJJA), May to July (MJJ), June to August (JJA), and September to December (SOND). At the yearly scale the sum (SumYear) and mean (MeanYear) of daily climate data were calculated. Following daily climate data were available or derived: average cloud fraction (CF, %), average relative humidity (RH, %), number of days with wind speed higher than 40 km/hour (WS, number of days), cumulative precipitation (P, mm), cumulative potential evapotranspiration (PET, mm), drought index (DRI = P-PET, mm), average maximum temperature (Tmax, ℃), average minimum temperature (Tmin, ℃), average temperature (Tav, ℃), and number of days with Tmin lower than −8 ℃ (frost, number of days). PET was calculated using the Thornthwaite (1948) equation based on Tav and latitude of the forest sites. For the period before 1952 data from the only available Belgian climatic station at Ukkel were used. Monthly difference between forest site inverse distance weighted climate data and Ukkel data for the period 1952–2014 was used to rescale Tmin, Tmax, Tav, P, RH and WS measured data in Ukkel before 1952.

Historical atmospheric deposition data of NHy (reduced nitrogen, DepNHy, kg/ha), NOx (oxidized nitrogen, DepNOx, kg/ha), SOx (oxidized sulfur, kg/ha), sum of DepNHy and DepNOx (nitrogen deposition, DepN, kg/ha), and phyto-toxic ozone doze (POD1, mmol/m²) were obtained from the EMEP dataset (Vieno et al., 2014). CO₂ (ppm) concentration data modelled for the northern hemisphere based on NOAA and AGAGE station data in combination with literature data were used (Meinshausen et al., 2016). The atmospheric deposition and CO₂ data are available for the entire modeling period (i.e. 1925–2014 and 1927–2014, for oak and beech respectively).

2.2.4. Detection of long-term trends in radial growth, wood density and biomass increment

Multilevel mixed models were used to model the long-term trends in radial growth, wood density and above-ground biomass increment. BAI was used as a proxy for stem increment:

$$BAI_t = \pi(R_t^2 - R_{t-1}^2)$$

where R is the tree radius at the end of the growing season (derived from cumulative TRW measurements) and t the year of ring formation. Above-ground biomass increment was estimated by an indicator for above-ground biomass increment (IAB, g/cm), which was calculated as the product of BAI and wood density at a yearly resolution for each cored tree. Since it was demonstrated by Bontemps et al. (2010) that

long-term trends in radial growth are similar with trends in height growth, the height dimension of above-ground biomass increment was not taken into account.

For both beech and oak the same modeling strategy was applied on BAI, wood density and IAB (hereafter referred to as response variables). A natural log (ln) transformation of BAI and IAB data was needed to deal with the heavily skewed distribution. The first thirty years of response variables for each tree were eliminated from the analysis to exclude the juvenile developmental stage. When including juvenile growth the comparison of trees at a different developmental stage in a specific year is difficult, given that juvenile growth can be suppressed which was the case in part of the cored trees (Jump et al., 2006). In addition, modeling was started from the year for which data from at least ten trees were available (1936 and 1925 for beech and oak, respectively).

Models were built in three stages according to Kint et al. (2012) and Aertsen et al. (2014) (i) **base model (Mb):** describes response variable as a function of tree development stage accounting for forest structure and site quality, (ii) **date model (Md):** examines a possible common source of variability related to calendar year, and (iii) **environmental model (Me):** tests if climatic or other environmental variables can explain the inter annual and/or long-term variability. The previous-year diameter (Dp, cm) was used as a proxy for developmental stage, since it is known to be a better proxy for developmental stage compared to cambial age (Wykoff, 1990; Mencuccini et al., 2005; Bontemps et al., 2009). For the response variables, the relationship with Dp was described by adding a linear (Dp) and quadratic (Dp²) effect of Dp. Only the significant effects were retained in the final models.

For the first modeling step (**base model**), forest structural and site quality variables were selected a priori using a multiple linear regression (only these forest structural and site quality variables with the criteria variance inflation factor < 5 and Pearson correlation > 0.75 with the response variable were considered) (Zuur et al., 2009). The selected forest structural and site quality variables for each response variable for both beech and oak are presented in Table S2 (see Supplementary material).

Next, the methodology of Zuur et al. (2009) was applied to determine the optimal random and fixed effect structure. The optimal random structure was determined by comparing nested models with random intercept for forest site and tree; and random slope for Dp and Dp² (restricted maximum likelihood (REML) fitted models). Then, a backward elimination of fixed effects (i.e. Dp, Dp² and selected forest structural and site quality variables) was used. A second-order autoregressive covariance structure for the error terms was added to the model in order to deal with the autocorrelation present in the data (i.e. growth and wood density in year t is related with year t-1). By doing this, the estimates and confidence intervals of the model parameters are not affected by the autocorrelation of the data (Pinheiro and Bates, 2000; Martin-Benito et al., 2011). The result of this first modeling step are three base models (i.e. BAI, wood density and IAB) for both beech and oak describing response variables in function of tree developmental stage (characterized by including Dp and/or Dp²) and local conditions (characterized by forest structure and site quality variables). As the base models are an intermediate modeling step they are not reported in this paper.

$$Mb: \ response_{fs,i,t} = \alpha + \beta\ T_{i,t} + \gamma\ F_i + \delta\ S_i + a_i + b_i T_{i,t} + c_{fs} + d_{fs}T_{i,t} + \xi_{fs,i} \tag{1}$$

where response$_{fs,i,t}$ is the response of tree i in year t located in forest site fs; $T_{i,t}$ is a vector related to the tree's development stage (Dp and/or Dp²). By including this in both fixed and random parts, both common and individual tree growth trajectories are modeled; α and β are intercept and slope related to $T_{i,t}$; a_i and b_i are tree specific random intercept and slope related to $T_{i,t}$; c_{fs} and d_{fs} are forest site specific random intercept and slope related to $T_{i,t}$; F_i and S_i are the vectors of the

preselected forest structural variables and site quality variables; γ and δ are the associated fixed effect estimates related to F_i and S_i; and finally $\xi_{fs,i}$ is the error term.

Changes of the response variable through time caused by overall long-term trends were not included in the base models. Therefore, in the second modeling step (**date model**) it was tested if a linear, quadratic, cubic or natural cubic spline term of calendar year could be added as a fixed effect to the base models.

$$\text{Md: } Md = Mb + \lambda\, Y_i \tag{2}$$

where λ is the vector of fixed effects estimated associated to calendar year. The date model allowed studying overall long-term trends in the response variables caused by exogenous factors operating at a broad geographical scale.

Climate and emission variables can explain year-to-year and/or long-term variability of the response variables. Therefore in the third modeling step (**environmental model**) climate and emission variables were added as fixed effects to the date models of BAI, wood density and above-ground biomass increment. This modelling step allowed seeing which climatic conditions affect radial growth, wood density and above-ground biomass increment.

$$\text{Me: } Me = Md + \mu\, C_{i,t} + \theta\, Ct_{i,t} + \vartheta\, O_{i,t} \tag{3}$$

where $C_{i,t}$ is a vector of climate variables characterizing the year-to-year changes in climatic conditions of current year and previous year (PY). A priori, possible $C_{i,t}$ variables were selected by selecting those variables that have a significant correlation with detrended BAI, wood density and IAB data, respectively. $Ct_{i,t}$ is a vector of climate variables characterizing the long-term changes in climate conditions. $Ct_{i,t}$ was calculated for the a priori selected climate variables (i.e. $C_{i,t}$ variables) by applying a local smoothing function (loess, with polynomial degree = 1) to the considered climate variables. $O_{i,t}$ is a vector with emission variables: DepNHy, DepNOx, DepN, DepSOx, DOP and CO_2. Vectors μ, θ and ϑ gives the fixed effects associated with $C_{i,t}$, $Ct_{i,t}$ and $O_{i,t}$, respectively. It can be that in this final modeling step the fixed effect Y becomes no longer significant, indicating that $C_{i,t}$, $Ct_{i,t}$ and $O_{i,t}$ are driving changes in the response variable.

For beech, an additional model for wood density was built in order to test if wood density changes independently of radial growth changes. This was done by building a mixed model of wood density with an interaction of ln(BAI) and Dp as fixed factor, a random intercept for tree and a random slope for ln(BAI):Dp. Similarly as in the date models, a second order autocorrelation structure was added to account for the

autocorrelation present in the data. In a second step, we tested if a linear, quadratic, cubic or natural cubic spline term of calendar year could be added to the model. Since no long-term changes in wood density were found for oak we did not build such a model for that species.

For the selection of the optimal fixed and random effect structure, a likelihood ratio test was applied to nested models and Akaike and Bayesian Information criteria (AIC and BIC) were compared. Final models were fitted with restricted maximum likelihood (REML) and their model performance was evaluated with pseudo-R^2 of full and marginal model (i.e. only considering fixed effects) and relative root mean squared error (rRMSE, calculated for response). The pseudo-R^2 was calculated as the correlation between the response and model predictions. All statistics were performed in R (version 3.2.5) (R Development Core Team, 2016) with packages "nlme", "spline" and "dplr" (Bunn, 2008; Hothorn et al., 2008; Pinheiro et al., 2016).

3. Results

3.1. General statistics

In Table 2 general statistics of measured TRW and wood density is summarized. The TRW of beech trees is greater compared to oak (p-value < 0.001). Also, the average wood density is higher in beech trees compared to oak (p-value < 0.001). Table S1 gives an overview of some forest structure and site quality variables for the four forest sites for both beech and oak.

3.2. Models

Pearson correlation between the random components and tree age are not significant (p-value > 0.001) for all the models. This guarantees that the tree age effect on the response variables is well captured by adding Dp as a fixed effect in the models. A significant correlation between random components and tree age would indicate that the response variable is modelled differently for trees with different age which could obscure part of the long-term trend.

3.3. Date models

The parameter estimations and model evaluation of the date models, which describe long-term variability of BAI, wood density and IAB with calendar year, for both beech and oak are presented in Tables 3 and 4, respectively. A random intercept for tree and a random slope

Table 3
Parameter estimates and model evaluation of the date models with response variables ln(BAI), wood density and ln(IAB) for beech.

Fixed effects	ln(BAI), [cm²] (n = 2241)				wood density, [kg/m³] (n = 2226)				ln(IAB), [g/cm] (n = 2226)			
	Estimate	SE	Df	p > |t|	Estimate	SE	Df	p > |t|	Estimate	SE	Df	p > |t|
(Intercept)	−10.0804	3.8485	2196	0.0089	2384730.5	1019802.6	2180	0.0195	−13.3262	4.3325	2181	0.0021
Dp	0.0869	0.0086	2196	< 0.0001	−1.3	0.5	2180	0.0055	0.0876	0.0092	2181	< 0.0001
Dp²	−0.0009	0.0001	2196	< 0.0001					−0.0009	0.0001	2181	< 0.0001
C/N	−0.0572	0.0172	40	0.0019					−0.0555	0.0194	40	0.0067
year	0.0063	0.0019	2196	0.0011	−3630.4	1547.2	2180	0.0190	0.0077	0.0022	2181	0.0003
year²					1842.5	782.4	2180	0.0186				
year³					−0.3	0.1	2180	0.0182				

Random effect tree	Intercept	Dp	error	Intercept	Dp	error	Intercept	Dp	error
	0.6575	0.0182	0.4101	45.8376	1.6407	29.6230	0.6897	0.0201	0.4320

Model evaluation	R²f	R²m	rRMSE	AIC	R²f	R²m	rRMSE	AIC	R²f	R²m	rRMSE	AIC
	0.67	0.38	12%	1945	0.68	0.11	4%	20712	0.64	0.30	15%	2125

BAI (basal area increment), IAB (indicator for above-ground biomass increment), Dp (previous year diameter, cm), C/N (ratio C/N measured in soil sample), year² is (year²/1000), year³ is (year³/1000), R²f (pseudo- R^2 of the full model), R²m (pseudo- R^2 of the marginal model), rRMSE (relative root mean squared error) and AIC (Akaike Information Criteria).

Table 4

Parameter estimates and model evaluation of the date models with response variables ln(BAI), wood density and ln(IAB) for oak.

Fixed effects	ln(BAI), [cm²] (n = 2937)				wood density, [kg/m³] (n = 2922)				ln(IAB), [g/cm] (n = 2876)			
	Estimate	SE	Df	p > |t|	Estimate	SE	Df	p > |t|	Estimate	SE	Df	p > |t|
(Intercept)	28373.727	6317.938	2888	< 0.0001	728.6196	9.3866	2877	< 0.0001	28042.662	7174.0800	2828	0.0001
Dp	0.06	0.009	2888	< 0.0001	−2.3596	0.3107	2877	< 0.0001	0.0635	0.0100	2828	< 0.0001
Dp²	−0.001	0.0001	2888	< 0.0001					−0.0008	0.0002	2828	< 0.0001
BAL	−0.275	0.078	42	0.0010								
OC									−0.0870	0.0240	41	0.0009
year	−43.09	9.608	2888	< 0.0001					−42.5455	10.9110	2828	0.0001
year²	21.81	4.870	2888	< 0.0001					21.5136	5.5310	2828	0.0001
year³	−0.004	0.001	2888	< 0.0001					−0.0036	0.0010	2828	0.0001

Random effect tree	Intercept	Dp	error	Intercept	Dp	error	Intercept	Dp	error
	0.7406	0.0242	0.3335	41.4709	1.5101	46.9754	0.7212	0.0274	0.3868

Model evaluation	R²f	R²m	rRMSE	AIC	R²f	R²m	rRMSE	AIC	R²f	R²m	rRMSE	AIC
	0.64	0.13	11%	1196	0.605	0.093	7%	30016	0.57	0.00067	15.00%	2063

BAI (basal area increment), IAB (indicator for above-ground biomass increment), Dp (previous year diameter, cm), BAL (basal area of trees larger than cored tree, m²), OC (soil organic C, %), year² is (year²/1000), year³ is (year³/1000), R^2f (pseudo- R^2 of the full model), R^2m (pseudo- R^2 of the marginal model), rRMSE (relative root mean squared error) and AIC (Akaike Information Criteria).

associated with Dp was identified as the optimal random structure for the three response variables for both studied tree species. Since for none of the models the random intercept forest site improved the model performance, it is not included in the models. For both beech and oak wood density models, a negative estimate is associated with fixed effect Dp, indicating that wood density decreases as the tree matures, in line with the increased tree height and hydraulic system requirements (Fig. S2). Adding Dp^2 as a fixed effect to the density models of both beech and oak did not improve the model and is thus not included in the final models. A quadratic relation with tree developmental stage with BAI and IAB is given by the positive and negative estimates for Dp and Dp^2. This is expected as tree growth is known to increase until a certain maximum is reached, whereafter tree growth starts to decline (Fig. S2). The site quality variable C/N is included as a fixed effect in the date models for BAI and IAB for beech. The associated negative effect indicates that both BAI and IAB of beech decreases with higher soil C/N values. For oak, the forest structural variable BAL is included in the BAI date model with a negative estimate, reflecting a competition effect on radial growth. In the IAB date model for oak, site quality variable OC is included in the model with a negative estimate, oak trees growing on soils with higher OC content have thus a lower IAB. No forest structural or site quality variables are included as fixed effects in the beech and oak date model for wood density. Thus, other variables are driving wood density in both tree species.

The overall (i.e. for all trees) long-term effect of calendar year on response variables as described by the date models, can be visualized by plotting the response through time under constant growth conditions (site quality and forest structural variables, if any included as fixed effects) and for a fixed developmental stage (for beech and oak median values from 1936 and 1925 respectively are taken), see full line in Figs. 1 and 2. Note that by including Dp as a fixed effect in the models, the effect of increasing number of older trees with time in the dataset and their higher radial growth and lower wood density (compared to younger trees) is filtered out. The random effect Dp will allow the relationship between growth-Dp and wood density-Dp to vary for each tree. This modeling strategy assures that the detected long-term effect of calendar year is minimally influenced by effects of the tree's developmental stage (Dp).

Year is included as a fixed effect with a positive estimate in the BAI date model of beech, beech BAI increased 63.2% in the study area for the period 1936 and 2014. In the wood density model for beech a cubic effect of calendar year indicates a minimal decrease (−0.35%, wood

density 1946 relative to 1936) in wood density until 1946, afterwards wood density increases slightly (2.8%, wood density in 1996 relative to 1946) with a maximum reached in 1996. From 1996 onwards wood density starts to decline again, in 2014 the same wood density as in 1958 is reached. Overall wood density of beech increases with 1.1% during the period between 1936 and 2014. As expected, since for both BAI and wood density a long-term increase was found, IAB of beech also increases for the period 1936 and 2014. The estimate of year in the IAB model is higher compared to the BAI model. Overall, an increase of beech IAB of 82.9% was found for the period 1936–2014.

For oak, a cubic effect of calendar year is included in the models of BAI and IAB. BAI and IAB decreased until the 1950's; afterwards they increased until the 2000's whereafter they decline again. Note that the estimates of the cubic effect of calendar year are very similar for the models of BAI and IAB. Overall, an increase of oak BAI of 9.3% and a slight decrease of IAB −1.9% was found for the period 1925–2014. Since year is not included in the optimal wood density model no overall long-term trend in wood density is found in oak trees.

The R^2f (pseudo-R^2 of the full model) of date models are relatively high, indicating a good fit. The pseudo-R^2 of the marginal models, R^2m, are low indicating that the fixed effects could not explain a large part of the variability of the response variables and it was thus captured by the random effects. This is particularly the case for the wood density and IAB date model of oak. The rRMSE is comparable and acceptably low for all six models. Note that the number of observations is lower in the wood density model; this is because some rings were too small to measure wood density accurately or because of mineral inclusions in some rings which influence the measured wood density (Vansteenkiste et al., 2007).

The estimates and model performance of the beech wood density model where radial growth change is taken into account are presented in Table 5. In Fig. 3 the model is visualized, the full line represents the modelled change in wood density through time for a tree with fixed Dp and BAI (median values of Dp and ln(BAI) values from 1936 are taken). A decrease in wood density of −6% is modelled from 1925 to 2014 for a tree with constant Dp and BAI (median values from 1936 are taken). Note that the value of the observed median wood density (dotted line) is slightly different compared to the wood density model presented in Fig. 1. This is because values are presented relative to the 1936 predicted wood density, which is different for the two models visualized in Figs. 1 and 3.
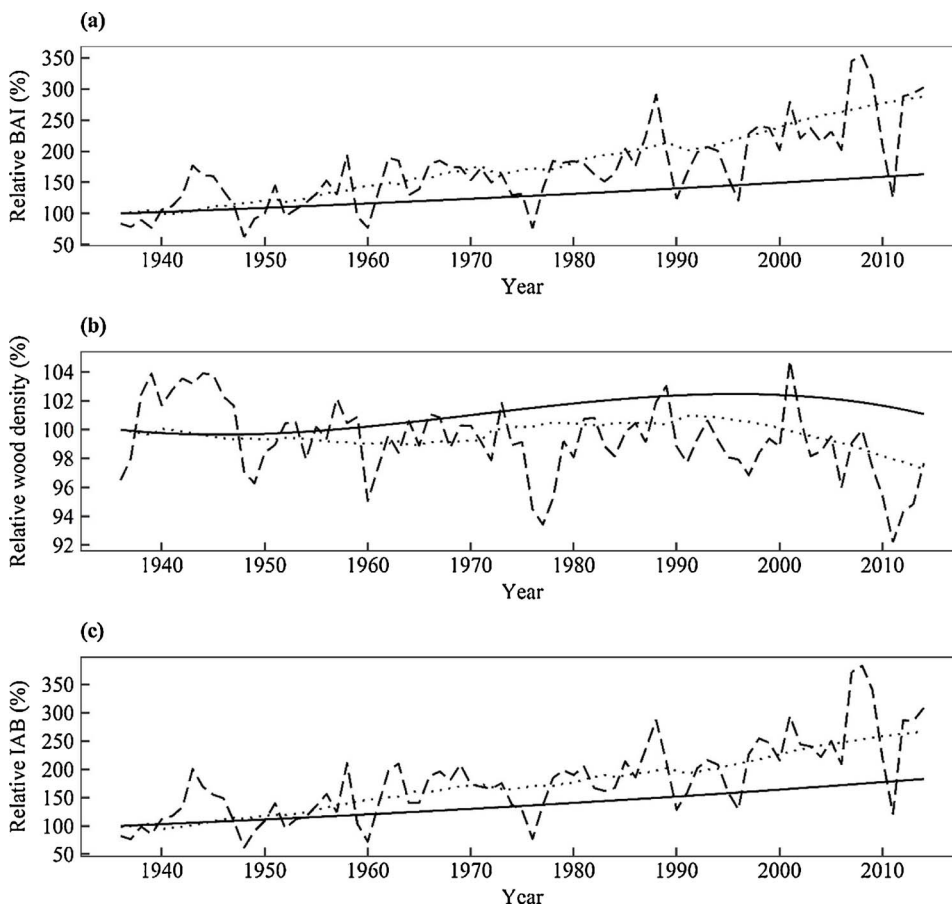
(a)

(b)

(c)

Fig. 1. Modelled 20th century change in BAI (a), wood density (b) and IAB (c) of beech, using the date model. The dashed line represents the observed median response variable (i.e. BAI, wood density and IAB). The dotted line represents the predicted response using median yearly predictor values. The full line represents the long-term trend of a tree with constant C/N (for BAI and IAB model) and Dp (median values from 1936 are taken). Values are presented relative to the 1936 predicted response values.

3.4. Environmental models

The result of the addition of environmental variables as fixed effects to the BAI and wood density models is presented in Tables 6 and 7, for beech and oak, respectively. Since for some climate variables observations are missing in some years, the number of observations of the environmental models is lower compared to the date models (Tables 3 and 4). No variables characterizing trends in climate variables ($Ct_{i,t}$) are included in the final environmental models. Only for the radial growth model of beech, inclusion of the environmental variables resulted in non-significance of the calendar year included in the date model. Though, for all models the addition of the environmental variables explains part of the year-to-year variation of the response variables resulting in better performing models compared to the date models (Tables 3 and 4 compared to Tables 6 and 7).

Positive estimates of CF in June (CF_June), DRI from January to March (DRI_JFM) and DRI from April to August (DRI_AMJJA) in the beech radial growth environmental model, indicate that beech radial growth is negatively affected by drought during the growing season and dormant season. Besides, the inclusion of: Tmax in July of the previous year (PY_Tmax_July), P from May to July of the previous year (PY_P_MJJ), RH of the previous year (PY_RH_MeanYear) and CF from June to August of the previous year (PY_CF_JJA) indicates that current year radial growth is affected by previous year drought conditions. CO_2 and POD1 are included with a positive and negative estimate in the beech radial growth environmental model, respectively. The variables included in the beech wood density environmental model with a positive estimate are: CF in March of the previous year (PY_CF_March), DRI from May to July of the previous year (PY_DRI_MJJ) and P in October of the previous year (PY_P_October). PET from June to August in the previous year (PY_PET_JJA) and DepN are included with a negative estimate in the beech wood density environmental model.

For oak, the radial growth is positively influenced by P from January to August (P_JFMAMJJA), Tav in May (Tav_May), Tmin in May of the previous year (PY_Tmin_May) and DepNOx, and negatively by the number of days where Tmin is lower than −8 °C in February (frost_February). In the oak wood density environmental model, frost_February is also included with a negative estimate as well as the number of days where Tmin is lower than −8 °C in February of the previous year (PY_frost_February). P in April (P_April), cumulative P of the previous year (PY_P_SumYear), RH in May of the previous year (PY_RH_May) and Tmax in February (Tmax_February) positively influence oak wood density. The environmental IAB models contain similar climatic variables as the wood density and BAI environmental models for beech and oak, which is expected since IAB is calculated as the product of BAI and wood density (for the IAB environmental models, see Supplementary material Tables S3 and S4).

4. Discussion

4.1. Long-term radial growth, wood density and above-ground biomass increment trends in beech

For beech growing on the Ardennes plateau, a long-term radial growth increase (63.2%) is observed during the period between 1936 and 2014 (Fig. 1 and Table 3). This is in contrast with the recent radial growth decline detected since the 1960s in beech trees growing in the North of Belgium by Kint et al. (2012), but is in line with studies in other European upland regions (Lorraine, Vosges mountains, Middle and Central Germany, Albania and Macedonia in Badeau et al., 1996; Bontemps and Esper, 2011; Pretzsch et al., 2014; Tegel et al., 2014). Drought and high N deposition were identified as drivers of growth decline of beech growing in the densely populated lowland of Flanders, North of Belgium (Kint et al., 2012), and compared to this area, the
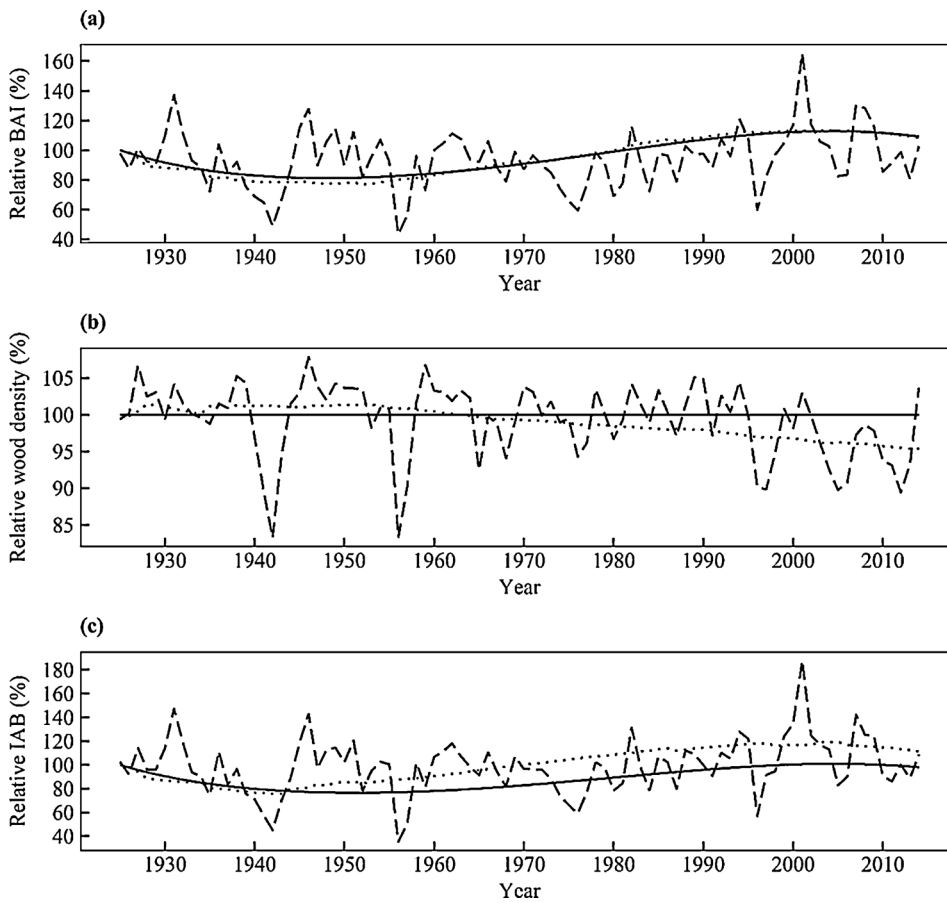
Fig. 2. Modelled 20th century change in BAI (a), wood density (b) and IAB (c) of oak, using the date model. The dashed line represents the observed median response variable (i.e. BAI, wood density and IAB). The dotted line represents the predicted response using median yearly predictor values. Full line represents the long-term trend of a tree with constant BAL and OC (for BAI and IAB model respectively) and Dp (median values from 1925 are taken). Values are presented relative to the 1925 predicted response values.

Belgian Ardennes have more rainfall and higher summer air humidity, and received less N deposition over time. It seems that for the time being, beech trees in the Ardennes mainly took profit from global change through improved levels of CO_2 concentration, air temperature and nitrogen nutrition. Also a long-term increase of IAB (82.9%) is observed (Fig. 1 and Table 3) for that same period, which is substantially higher than the modelled long-term increase in radial growth (63.2%). This higher long-term increase is also suggested by the higher estimate for the calendar year effect in the IAB compared to the BAI model (year in Table 3). The observed increase in IAB is mostly

attributable to the increase in radial growth (63.2%), rather than to the much lower increase in wood density (1.1%) when looking at the period 1936–2014. Nevertheless, the results show that ignoring wood density changes leads to a substantial underestimation of long-term trends in IAB.

Wood density of a tree ring with a particular BAI decreases over time (see Table 7 and Fig. 3). For a tree at a fixed Dp and BAI, a decrease in wood density of −6% is modelled. This is in line with Bontemps et al. (2013) who also reported a decreasing trend of the same magnitude (−7.5%) on beech trees in France at constant ring

Table 5
Parameter estimates and model evaluation of the wood density model for beech where the interaction of ln(BAI) with Dp is included as a fixed effect.

Fixed effects	wood density beech, [kg/m³] (n = 2226)			
	Estimate	SE	Df	p > |t|
(Intercept)	2112857.2000	966086.8000	2178	0.0288
ln(BAI)	9.5000	3.7000	2178	0.0100
Dp	−2.4000	0.4000	2178	0.0000
year	−3212.4000	1465.6000	2178	0.0285
year²	1628.7000	741.1000	2178	0.0281
year³	−0.3000	0.1000	2178	0.0277
ln(BAI):Dp	0.4000	0.1000	2178	0.0000

Random effects	Intercept		log(BAI):Dp	error
	36.5043		0.1232	27.5786

Model evaluation	R²f	R²m	rRMSE	AIC
	0.72	0.21	4%	20366

BAI (basal area increment), Dp (previous year diameter), year² is (year²/1000) and year³ is (year³/1000), R²f (pseudo- R² of the full model), R²m (pseudo- R² of the marginal model), rRMSE (relative root mean squared error) and AIC (Akaike Information Criteria).
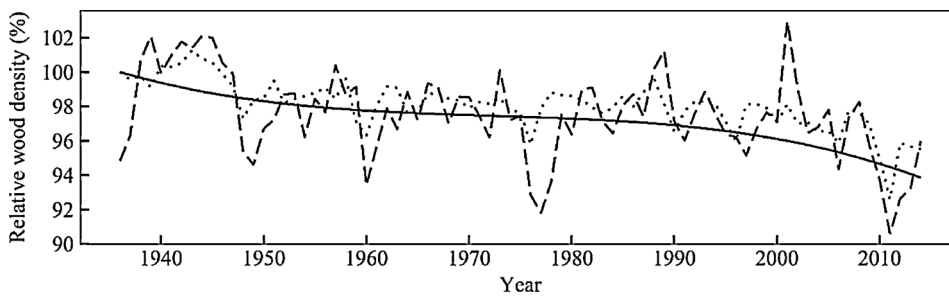
Fig. 3. Visualization of beech wood density model with radial growth change taken into account. The dashed line represents the observed median wood density. The dotted line represents the predicted wood density using median yearly predictor values. Full line represents the long-term trend of a tree with constant ln(BAI) and Dp (median values from 1936 are taken). Presented values are relative to the 1936 predicted wood density values.

width and tree radius. These findings suggest that an anatomical shift in wood formation driven by changes in the environment took place over time. An anatomical shift can be caused by changes in the composition of wood or a change in cell arrangements and characteristics (Bergès et al., 2000; Fonti et al., 2010). However, the decrease in wood density for tree-rings with a fixed BAI does not result in a long-term decrease in wood density over time. Overall wood density of beech trees increases (1.1%) for the period between 1936 and 2014.

4.2. Climatic factors influencing radial growth and wood density of beech

The environmental model, where environmental factors are added to the models that describe variability of BAI and wood density with calendar year, indicates that beech radial growth is limited by water availability (influenced by P and soil properties) and drought (resulting from a combination of low P, high T and low RH over a prolonged period) (Table 6). This is not surprising since beech is known to be sensitive to water availability and drought (Jump et al., 2006; Piovesan et al., 2008; Charru et al., 2010; Scharnweber et al., 2011; van der Maaten, 2012; Michelot et al., 2012; Kint et al., 2012). Note that the negative effect of drought and water shortage increases with increasing tree size (Rötzer et al., 2017). Köcher et al. (2009) has shown a decrease in sap flux and leaf water potential during drought in beech trees. The negative effect of previous year drought on radial growth can be explained by the dependency of current year growth on the carbohydrate

reserve (Skomarkova et al., 2006; Richardson et al., 2013). The negative effect of previous year drought or water availability on wood density of beech (Table 6) can be explained by the decrease in soluble carbohydrate reserve in the years following drought. Overall, the year-to-year variability in wood density is more determined by the previous year weather conditions, while radial growth is more determined by current year climate variables (Table 6).

The climate variables related to drought or water availability included in the environmental model of beech radial growth and wood density are not included as trends, indicating that they mainly explain the year-to-year variability in growth and wood density. Since a positive growth trend was detected, the negative effect of drought is currently overcompensated by other external factors that enhance radial growth, though this might change in the future since drought events will increase due to climate change (IPCC, 2013). Current and expected trends of the climate variables included in the models are indicating that drought might negatively affect radial growth and wood density of beech in the future (Tricot et al., 2015). Especially for PY_RH_MeanYear, which is included in the growth model with a positive estimate, a clear decreasing trend through time is visible, which might negatively affect growth in the future (see Fig. S3., Supplementary material). When BAI and wood density are combined (i.e. environmental model of IAB), we already see the negative effect of decreasing trend in RH on IAB (negative estimate for Trend_RH_MeanYear in Table S3).

The increasing trend in POD1 and CO_2 is influencing beech radial

Table 6
Parameter estimates and model evaluation of the environmental models with response variables ln(BAI) and wood density for beech.

ln(BAI), [cm²] (n = 2220)					wood density, [kg/m³] (n = 2222)				
Fixed effects	Estimate	SE	Df	p > |t|	Fixed effects	Estimate	SE	Df	p > |t|
(Intercept)	−2.3990	0.7142	2167	0.0008	(Intercept)	3926006	1034560.00	2171	0.0002
Dp	0.1000	0.0090	2167	< 0.0001	Dp	−1.3130	0.4670	2171	0.0050
Dp²	−0.0010	0.0001	2167	< 0.0001	year	−5988.766	1570.6578	2171	0.0001
C/N	−0.0536	0.0156	40	0.0014	year²	3045.164	794.8123	2171	0.0001
CF_June	0.0093	0.0007	2167	< 0.0001	year³	−0.516	0.1341	2171	0.0001
DRI_JFM	0.0004	0.0001	2167	< 0.0001	PY_CF_March	0.2453	0.0445	2171	< 0.0001
DRI_AMJJA	0.0009	0.0001	2167	< 0.0001	PY_DRI_MJJ	0.075	0.0064	2171	< 0.0001
PY_P_MJJ	0.0006	0.0001	2167	< 0.0001	PY_P_October	0.0411	0.0104	2171	0.0001
PY_Tmax_July	−0.0190	0.0039	2167	< 0.0001	PY_PET_JJA	−0.1469	0.0279	2171	< 0.0001
PY_RH_MeanYear	0.0128	0.0044	2167	0.0039	DepN	−1.3812	0.3085	2171	< 0.0001
PY_CF_JJA	0.0118	0.0014	2167	< 0.0001					
CO₂	0.0074	0.0013	2167	< 0.0001					
POD1	−0.0212	0.0051	2167	< 0.0001					

Random effects	Intercept	Dp	error	Random effects	Intercept	Dp	error
	0.6810	0.0188	0.3818		49.7102	1.7401	28.4921

Model evaluation	R²f	R²m	rRMSE	AIC	Model evaluation	R²f	R²m	rRMSE	AIC
	0.72	0.44	11%	1470		0.71	0.12	4%	20388

BAI (basal area increment), Dp (previous year diameter, cm), C/N (ratio C/N measured in soil sample), year² is (year²/1000) and year³ is (year³/1000), PY (previous year), CF (cloud fraction, %), P (precipitation, mm), PET (potential evapotranspiration, mm), DRI (P-PET, mm), Tmax (maximum temperature, ℃), RH (relative humidity, %), CO_2 (ppm), POD1 (phytotoxic ozone doze, mmol/m²), DepN (sum reduced and oxidized N deposition on deciduous trees, kg/ha), JFM (January to March), AMJJA (April to August), MJJ (May to July), JJA (June to August), R²f (pseudo- R² of the full model), R²m (pseudo- R² of the marginal model), rRMSE (relative root mean squared error) and AIC (Akaike Information Criteria).

Table 7

Parameter estimates and model evaluation of the environmental models with response variables ln(BAI) and wood density for oak.

ln(BAI), [cm^2] (n = 2936)					wood density, [kg/m^3] (n = 2901)				
Fixed effects	Estimate	SE	Df	p > |t|	Fixed effects	Estimate	SE	Df	p > |t|
(Intercept)	20989.7130	7258.2020	2882	0.0039	(Intercept)	581.1278	14.6568	2850	< 0.0001
Dp	0.0597	0.0090	2882	< 0.0001	Dp	−2.4990	0.3215	2850	< 0.0001
Dp^2	−0.0008	0.0000	2882	< 0.0001	frost_February	−0.7377	0.2021	2850	0.0003
BAL	−0.3012	0.0790	42	0.0004	P_April	0.0994	0.0178	2850	< 0.0001
year	−31.7929	11.0670	2882	0.0041	PY_frost_February	−1.0317	0.1356	2850	< 0.0001
year^2	16.0502	5.6250	2882	0.0044	PY_P_SumYear	0.0235	0.0041	2850	< 0.0001
year^3	−0.0027	0.0010	2882	0.0046	PY_RH_May	1.5558	0.1279	2850	< 0.0001
P_JFMAMJJA	0.0004	0.0000	2882	< 0.0001	Tmax_February	2.0962	0.3431	2850	< 0.0001
frost_February	−0.0064	0.0010	2882	< 0.0001					
Tav_May	0.0418	0.0030	2882	< 0.0001					
PY_Tmin_May	0.0443	0.0040	2882	< 0.0001					
DepNOx	0.0205	0.0080	2882	0.0078					

Random effects	Intercept	Dp	error	Random effects	Intercept	Dp	error
	0.739	0.024	0.311		41.476	1.574	44.237

Model evaluation	R^{2}f	R^{2}m	rRMSE	AIC	Model evaluation	R^{2}f	R^{2}m	rRMSE	AIC
	0.70	0.14	10%	878		0.66	0.13	7%	29425

BAI (basal area increment), Dp (previous year diameter, cm), BAL (basal area trees larger then target tree, m^2), year^2 is (year^2/1000) and year^3 is (year^3/1000), PY (previous year), P (precipitation, mm), frost_February (number of days in February where minimum temperature is below −8 ˚C), Tmin (minimum temperature, ˚C), Tmax (maximum temperature, ˚C), RH (relative humidity, %), DepNOx (oxidized N deposition on deciduous trees, kg/ha), JFMAMJJA (January to August), SumYear (cumulative sum for each year), R^{2}f (pseudo- R^2 of the full model), R^{2}m (pseudo- R^2 of the marginal model), rRMSE (relative root mean squared error) and AIC (Akaike Information Criteria).

growth negatively and positively, respectively (Table 6). The negative effect of POD1 on beech radial growth was expected since the critical POD1 level of 4 mmol/m^2 for beech as determined by Mills et al. (2011) was exceeded in the four forest sites since 1936. Negative effects of ozone concentration on the radial growth of beech, caused by cellular damage of ozone and consequently reducing biomass production, has already been demonstrated (Matyssek et al., 2010; Ainsworth et al., 2012). An ozone fumigation experiment by Pretzsch et al. (2010), demonstrated that even the annual radial growth, allocation pattern and stem form of beech trees is altered when double of the ambient ozone concentration is fumigated, resulting in a decreases of 10.2 m^3/ha/y in biomass increment for beech. Since the fixed effect of year was no longer significant in the environmental model, compared to the date model, this suggests that the rising CO_2 is causing the increase in radial growth of beech trees over time (Tables 3 and 5). However, the increasing radial growth is probably the result of direct and indirect effects of increased CO_2. The fertilization effect of CO_2 on tree growth is complex since factors as increased drought, nutrient limitation and acclimatization to elevated CO_2 might alleviate the CO_2 fertilization effect (Körner et al., 2005; Peñuelas et al., 2011; Ainsworth et al., 2012). Note that also stand density might have changed over time and may explain the observed positive long-term trend in BAI, unfortunately no data are available to test this.

The negative effect of DepN deposition on the wood density of beech can be caused by the effect N has on the xylem properties as was already demonstrated in some studies (Blaschke et al., 2002; Borghetti et al., 2017; Kostiainen et al., 2004). This negative effect of DepN on wood density might suggest that increasing DepN might affect carbon sequestration negatively in the future opposed to what is suggested by Magnani et al. (2007). On the other hand increasing DepN may result in a hydraulic structure that is more cavitation resistant which might be better in the long run (Borghetti et al., 2017). For the period 1936–2014 other environmental factors then DepN and CO_2 seem to influence the long-term trend in above-ground biomass increment of beech in the Belgian Ardennes (Table S3).

4.3. Long-term radial growth, wood density and above-ground biomass increment trends in oak

For oak, a radial growth decline of 18.7% is observed between 1925 and 1948 (Fig. 2). This radial growth decline is in line with other literature where extreme winter frost, drought and insect outbreaks were identified as growth decline drivers (Delatour, 1983; Thomas et al., 2002). From 1948–2004, radial growth increases with 31.7%, followed by another radial growth decline (3.7% from 2004 to 2014). No long-term trends are detected in wood density. A divergence between wood density and radial growth long-term trends was also observed by Bergès et al. (2000) on sessile oak in France. This divergence is also confirmed by Fig. S2, where no clear relationship between BAI and wood density is visible for oak. Though Bergès et al. (2000) found a long-term increase of radial growth in combination with a decrease in wood density and not a long-term increase of radial growth in combination with no long-term trends in wood density as is the case in this study. The observed long-term trend in IAB follows the same pattern as the observed long-term radial growth trend. From 1925–1951 a decrease (23.4%) in IAB is modelled, afterwards IAB increases again until 2005 (24.3% increase from 1951 to 2005). From 2005 onwards, IAB decreases again (2.8% decrease from 2005 to 2014). However, the long-term trend in BAI differs from IAB. From 1925–2014 an overall increase (9.3%) in oak radial growth is modelled opposed to a slight decrease (-1.9%) in IAB. The pattern of the long-term trend in IAB for oak is thus dominated by the long-term trend in oak radial growth but wood density affects the long-term trend in IAB.

4.4. Climatic factors influencing radial growth and wood density of oak

Compared to radial growth, wood density is more influenced by previous year and pre-growing season climate variables (Table 7) (for oak, the growing season starts around mid-April, Campioli et al., 2012). This can be explained by the dependence of current year earlywood formation on the carbohydrates reserves stored during previous year latewood formation (Richardson et al., 2013; Delpierre et al., 2016). Since no photo assimilates are present because oak tree growth starts

before bud burst this is the case here (Michelot et al., 2012; Kimak and Leuenberger, 2015). Unfavorable growth conditions in previous year thus result in low earlywood formation because of low availability of stored carbohydrates. Low earlywood formation affects the water transport negatively resulting in low latewood formation (with high density) which results in lower wood density (Pérez-de-Lis et al., 2016).

Late frost affects both BAI and wood density negatively, for wood density even the late frost of the previous year is influencing current year wood density (see fixed factors PY_frost_February and frost_February in Table 7). Also, the positive effect of maximum temperatures in February on wood density indicates the importance of the effect of late frost. Sessile oak is known to be vulnerable to embolism of large xylem vessels, with negative consequences for water flow, caused by late frost (Barbaroux and Bréda, 2002). Since oak tree growth starts before leaf unfolding, and thus no transpiration drives water flow yet, each spring, the water flow pathway needs to be reconstructed. Severe late frost will result in high embolism and thus requires large investments for water flow restoration resulting in lower growth and wood density (Barbaroux and Bréda, 2002).

Oak radial growth is positively influenced by precipitation from January to August, indicating that water availability has a positive effect on oak growth. This positive effect of water availability was also found in other studies on oak growth (Kelly et al., 2002; Kint et al., 2012). The positive effect of May temperatures of previous and current year on radial growth is in line with previous research (Lindner et al., 2010). Our results indicate that nitrogen has a positive effect on the growth of sessile oak (Table 7). This is in line with previous research that indicated that for deciduous trees in the south of Belgium the critical nitrogen load is not yet reached (Ceulemans and Nijs, 2004).

4.5. Consequences of trends in radial growth and wood density on above-ground biomass increment

For both beech and oak, the long-term variability in IAB is mostly driven by the variability in radial growth rather than the long-term trend in wood density. Though, the assumption that wood density is constant in most carbon sequestration studies is not correct and may result in over- or underestimation of C storage capacity of forests. For beech, models indicate that ignoring wood density in above-ground biomass increment estimation results in an underestimation of the long-term trend in above-ground biomass increment for the period 1936–2014. For oak, ignoring wood density in long-term above-ground biomass increment results in an overestimation of the stored above-ground biomass increment for the period 1925–2014. For both beech and oak the observed long-term trend in BAI is higher compared to the trend in wood density, which might suggest that climate change is impacting BAI more than wood density. The environmental models (Tables 6 and 7) indicate that different climate variables are influencing wood density and radial growth, where wood density is more influenced by previous year parameters, whereas radial growth is more influenced by current year climate. This finding supports recent research that suggest a lag between cell enlargement (influencing radial growth) and cell wall thickening (influencing wood density) and that these xylogenesis processes are influenced by different environment conditions and use stored carbohydrates which are also climate sensitive (Cuny et al., 2015; Delpierre et al., 2016; Guillemot et al., 2017; Pérez-de-Lis et al., 2017). Also forest age, which is influenced by the forest management, should be considered when assessing the carbon storage capacity of forests since both radial growth and wood density in both beech and oak are influenced indirectly by tree age (i.e. effect of Dp and Dp^2 in models). The negative relationship between wood density and Dp is the result of increasing tree height when trees age and not the result of tree aging per se. In order to maintain water supply the lumen area increases, resulting in a decrease in wood density, when trees grow taller (Carrer et al., 2015).

Appendix A. Supplementary data

Supplementary data associated with this article can be found, in the online version, at https://doi.org/10.1016/j.dendro.2018.02.001.

References

Aertsen, W., Janssen, E., Kint, V., Bontemps, J.-D., Van Orshoven, J., Muys, B., 2014. Long-term growth changes of common beech (Fagus sylvatica L.) are less pronounced on highly productive sites. For. Ecol. Manage. 312, 252–259. http://dx.doi.org/10.1016/j.foreco.2013.09.034.

Ainsworth, E.A., Yendrek, C.R., Sitch, S., Collins, W.J., Emberson, L.D., 2012. The effects of tropospheric ozone on net primary productivity and implications for climate change. Annu. Rev. Plant Biol. 63, 637–661. http://dx.doi.org/10.1146/annurev-arplant-042110-103829.

Babst, F., Poulter, B., Trouet, V., Tan, K., Neuwirth, B., Wilson, R., Carrer, M., Grabner, M., Tegel, W., Levanic, T., Panayotov, M., Urbinati, C., Bouriaud, O., Ciais, P., Frank, D., 2013. Site- and species-specific responses of forest growth to climate across the European continent. Glob. Ecol. Biogeogr. 22, 706–717. http://dx.doi.org/10.1111/geb.12023.

Babst, F., Bouriaud, O., Papale, D., Gielen, B., Janssens, I.A., Nikinmaa, E., Ibrom, A., Wu, J., Bernhofer, C., Köstner, B., Grünwald, T., Seufert, G., Ciais, P., Frank, D., 2014. Above-ground woody carbon sequestration measured from tree rings is coherent with net ecosystem productivity at five eddy-covariance sites. New Phytol. 201, 1289–1303. http://dx.doi.org/10.1111/nph.12589.

Badeau, V., Becker, M., Bert, D., Dupouey, J.L., Lebourgeois, F., Picard, J.-F., 1996. Long-term growth trends of trees: ten years of dendrochronological studies in France. Growth Trends in European Forests. Springer, pp. 167–181.

Barbaroux, C., Bréda, N., 2002. Contrasting distribution and seasonal dynamics of carbohydrate reserves in stem wood of adult ring-porous sessile oak and diffuse-porous beech trees. Tree Physiol. 22, 1201–1210. http://dx.doi.org/10.1093/treephys/22.17.1201.

Bergès, L., Dupouey, J.-L., Franc, A., 2000. Long-term changes in wood density and radial growth of Quercus petraea Liebl. in northern France since the middle of the nineteenth century. Trees 14, 398–408. http://dx.doi.org/10.1007/s004680000055.

Björklund, J., Seftigen, K., Schweingruber, F., Fonti, P., von Arx, G., Bryukhanova, M.V., Cuny, H.E., Carrer, M., Castagneri, D., Frank, D.C., 2017. Cell size and wall dimensions drive distinct variability of earlywood and latewood density in Northern Hemisphere conifers. New Phytol. 216, 728–740. http://dx.doi.org/10.1111/nph.14639.

Blaschke, L., Forstreuter, M., Sheppard, L.J., Polle, A., 2002. Lignification in beech (Fagus sylvatica) grown at elevated CO2 concentrations. Tree Physiol. 22, 469–477. http://dx.doi.org/10.1093/treephys/22.7.469.

Bontemps, J.-D., Esper, J., 2011. Statistical modelling and RCS detrending methods provide similar estimates of long-term trend in radial growth of common beech in north-eastern France. Dendrochronologia 29, 99–107. http://dx.doi.org/10.1016/j.dendro.2010.09.002.

Bontemps, J.-D., Hervé, J.-C., Dhôte, J.-F., 2009. Long-term changes in forest productivity: a consistent assessment in even-aged stands. For. Sci. 55, 549–564.

Bontemps, J.-D., Hervé, J.-C., Dhôte, J.-F., 2010. Dominant radial and height growth reveal comparable historical variations for common beech in north-eastern France. For. Ecol. Manage. 259, 1455–1463. http://dx.doi.org/10.1016/j.foreco.2010.01.019.

Bontemps, J.-D., Gelhaye, P., Nepveu, G., Hervé, J.-C., 2013. When tree rings behave like foam: moderate historical decrease in the mean ring density of common beech paralleling a strong historical growth increase. Ann. For. Sci. 70, 329–343. http://dx.doi.org/10.1007/s13595-013-0263-2.

Borghetti, M., Gentilesca, T., Leonardi, S., van Noije, T., Rita, A., Mencuccini, M., 2017. Long-term temporal relationships between environmental conditions and xylem functional traits: a meta-analysis across a range of woody species along climatic and nitrogen deposition gradients. Tree Physiol. 37, 4–17. http://dx.doi.org/10.1093/treephys/tpw087.

Bouriaud, O., Bréda, N., Moguédec, G.L., Nepveu, G., 2004. Modelling variability of wood density in beech as affected by ring age, radial growth and climate. Trees 18, 264–276. http://dx.doi.org/10.1007/s00468-003-0303-x.

Bouriaud, O., Teodosiu, M., Kirdyanov, A.V., Wirth, C., 2015. Influence of wood density in tree-ring based annual productivity assessments and its errors in Norway spruce. Biogeosci. Discuss. 12, 5871–5905. http://dx.doi.org/10.5194/bgd-12-5871-2015.

Briffa, K.R., Osborn, T.J., Schweingruber, F.H., Jones, P.D., Shiyatov, S.G., Vaganov, E.A., 2002. Tree-ring width and density data around the Northern Hemisphere: part 1, local and regional climate signals. Holocene 12, 737–757. http://dx.doi.org/10.1191/0959683602hl587rp.

Bunn, A.G., 2008. A dendrochronology program library in R (dplR). Dendrochronologia 26, 115–124. http://dx.doi.org/10.1016/j.dendro.2008.01.002.

Campioli, M., Vincke, C., Jonard, M., Kint, V., Demarée, G., Ponette, Q., 2012. Current status and predicted impact of climate change on forest production and bio-geochemistry in the temperate oceanic European zone: review and prospects for Belgium as a case study. J. For. Res. 17, 1–18. http://dx.doi.org/10.1007/s10310-011-0255-8.

Carrer, M., von Arx, G., Castagneri, D., Petit, G., 2015. Distilling allometric and environmental information from time series of conduit size: the standardization issue and its relationship to tree hydraulic architecture. Tree Physiol. 35, 27–33.

Ceulemans, R., Nijs, I., 2004. Global change impact on ecosystems. In: Den Ouden, Vanderstraeten, M. (Eds.), Belgian Global Change Research 1990–2002. Assessment and Integration Report. Belgian Science Policy, Brussels, pp. 135–171.

Charru, M., Seynave, I., Morneau, F., Bontemps, J.-D., 2010. Recent changes in forest productivity: An analysis of national forest inventory data for common beech (Fagus sylvatica L.) in north-eastern France. For. Ecol. Manage. 260, 864–874. http://dx.doi.org/10.1016/j.foreco.2010.06.005.

Ciais, P., Reichstein, M., Viovy, N., Granier, A., Ogée, J., Allard, V., Aubinet, M., Buchmann, N., Bernhofer, C., Carrara, A., 2005. Europe-wide reduction in primary productivity caused by the heat and drought in 2003. Nature 437, 529–533. http://dx.doi.org/10.1038/nature03972.

Cuny, H.E., Rathgeber, C.B.K. Frank, D., Fonti, P., Mäkinen, H., Prislan, P., Rossi, S., Castillo del, E.M., Campelo, F., Vavrčík, H., Camarero, J.J., Bryukhanova, M.V., Jyske, T., Gričar, J., Gryc, V., Luis, M.D., Vieira, J., Čufar, K., Kirdyanov, A.V., Oberhuber, W., Treml, V., Huang, J.-G., Li, X., Swidrak, I., Deslauriers, A., Liang, E., Nöjd, P., Gruber, A., Nabais, C., Morin, H., Krause, C., King, G., Fournier, M., 2015. Woody biomass production lags stem-girth increase by over one month in coniferous forests. Nat. Plants 1http://dx.doi.org/10.1038/nplants.2015.160. nplants2015160.

De Mil, T., Vannoppen, A., Beeckman, H., Van Acker, J., Van den Bulcke, J., 2016. A field-to-desktop toolchain for X-ray CT densitometry enables tree ringanalysis. Ann. Bot. 117, 1187–1196. http://dx.doi.org/10.1093/aob/mcw063n.

Delatour, C., 1983. Les dépérissements de chênes en Europe. Rev. For. 35, 265–282. http://dx.doi.org/10.4267/2042/21659.

Delpierre, N., Berveiller, D., Granda, E., Dufrêne, E., 2016. Wood phenology, not carbon input, controls the interannual variability of wood growth in a temperate oak forest. New Phytol. 210, 459–470. http://dx.doi.org/10.1111/nph.13771.

Fahey, T.J., Woodbury, P.B., Battles, J.J., Goodale, C.L., Hamburg, S.P., Ollinger, S.V., Woodall, C.W., 2010. Forest carbon storage: ecology, management, and policy. Front. Ecol. Environ. 8, 245–252. http://dx.doi.org/10.1890/080169.

Fonti, P., von Arx, G., García-González, I., Eilmann, B., Sass-Klaassen, U., Gärtner, H., Eckstein, D., 2010. Studying global change through investigation of the plastic responses of xylem anatomy in tree rings. New Phytol. 185, 42–53. http://dx.doi.org/10.1111/j.1469-8137.2009.03030.x.

Frank, D., Esper, J., 2005. Characterization and climate response patterns of a high-elevation, multi-species tree-ring network in the European Alps. Dendrochronologia 22, 107–121. http://dx.doi.org/10.1016/j.dendro.2005.02.004.

Grassi, G., House, J., Dentener, F., Federici, S., den Elzen, M., Penman, J., 2017. The key role of forests in meeting climate targets requires science for credible mitigation. Nat. Clim. Change 7, 220–226. http://dx.doi.org/10.1038/nclimate3227.

Grissino-Mayer, H.D., 2001. Evaluating crossdating accuracy: a manual and tutorial for the computer program COFECHA. Tree-Ring Res. 57 (2), 205–221.

Guillemot, J., Francois, C., Hmimina, G., Dufrêne, E., Martin-StPaul, N.K., Soudani, K., Marie, G., Ourcival, J.-M., Delpierre, N., 2017. Environmental control of carbon allocation matters for modelling forest growth. New Phytol. 214, 180–193. http://dx.doi.org/10.1111/nph.14320.

Holmes, R.L., 1983. Computer-assisted quality control in tree-ring dating and measurement. Tree-Ring Bull. 43, 51–67.

Hothorn, T., Bretz, F., Westfall, P., 2008. Simultaneous inference in general parametric models. Biom. J. 50, 346–363. http://dx.doi.org/10.1002/bimj.200810425.

IPCC, 2013. In: Stocker, T.F., Qin, D., Plattner, G.-K., Tignor, M., Allen, S.K., Boschung, J., Nauels, A., Xia, Y., Bex, V., Midgley, P.M. (Eds.), Climate Change 2013: The Physical Science Basis. Contribution of Working Group I to the Fifth Assessment Report of the Intergovernmental Panel on Climate Change. Cambridge University Press, Cambridge, United Kingdom and New York, NY, USA.

Jump, A.S., Hunt, J.M., Peñuelas, J., 2006. Rapid climate change-related growth decline at the southern range edge of Fagus sylvatica. Glob. Change Biol. 12, 2163–2174. http://dx.doi.org/10.1111/j.1365-2486.2006.01250.x.

Köcher, P., Gebauer, T., Horna, V., Leuschner, C., 2009. Leaf water status and stem xylem flux in relation to soil drought in five temperate broad-leaved tree species with contrasting water use strategies. Ann. For. Sci. 66, 101. http://dx.doi.org/10.1051/forest/2008076.

Körner, C., Asshoff, R., Bignucolo, O., Hättenschwiler, S., Keel, S.G., Peláez-Riedl, S., Pepin, S., Siegwolf, R.T.W., Zotz, G., 2005. Carbon flux and growth in mature deciduous forest trees exposed to elevated CO2. Science 309, 1360–1362. http://dx.doi.org/10.1126/science.1113977.

Kelly, P.M., Leuschner, H.H., Briffa, K.R., Harris, I.C., 2002. The climatic interpretation of pan-European signature years in oak ring-width series. Holocene 12, 689–694. http://dx.doi.org/10.1191/0959683602hl582rp.

Kimak, A., Leuenberger, M., 2015. Are carbohydrate storage strategies of trees traceable by early–latewood carbon isotope differences? Trees 29, 859–870. http://dx.doi.org/10.1007/s00468-015-1167-6.

Kint, V., Aertsen, W., Campioli, M., Vansteenkiste, D., Delcloo, A., Muys, B., 2012. Radial growth change of temperate tree species in response to altered regional climate and air quality in the period 1901–2008. Clim. Change 115, 343–363. http://dx.doi.org/10.1007/s10584-012-0465-x.

Kostiainen, K., Kaakinen, S., Saranpää, P., Sigurdsson, B.D., Linder, S., Vapaavuori, E.,

2004. Effect of elevated [CO2] on stem wood properties of mature Norway spruce grown at different soil nutrient availability. Glob. Change Biol. 10, 1526–1538. http://dx.doi.org/10.1111/j.1365-2486.2004.00821.x.

Lindner, M., Maroschek, M., Netherer, S., Kremer, A., Barbati, A., Garcia-Gonzalo, J., Seidl, R., Delzon, S., Corona, P., Kolström, M., Lexer, M.J., Marchetti, M., 2010. Climate change impacts, adaptive capacity, and vulnerability of European forest ecosystems. For. Ecol. Manage. 259, 698–709. http://dx.doi.org/10.1016/j.foreco.2009.09.023.

Luyssaert, S., Ciais, P., Piao, S.L., Schulze, E.-D., Jung, M., Zaehle, S., Schelhaas, M.J., Reichstein, M., Churkina, G., Papale, D., Abril, G., Beer, C., Grace, J., Loustau, D., Matteucci, G., Magnani, F., Nabuurs, G.J., Verbeeck, H., Sulkava, M., Van Der WERF, G.R., Janssens, I.A., members of the CARBOEUROPE-IP SYNTHESIS TEAM, 2010. The European carbon balance. part 3: forests. Glob. Change Biol. 16, 1429–1450. http://dx.doi.org/10.1111/j.1365-2486.2009.02056.x.

Magnani, F., Mencuccini, M., Borghetti, M., Berbigier, P., Berninger, F., Delzon, S., Grelle, A., Hari, P., Jarvis, P.G., Kolari, P., Kowalski, A.S., Lankreijer, H., Law, B.E., Lindroth, A., Loustau, D., Manca, G., Moncrieff, J.B., Rayment, M., Tedeschi, V., Valentini, R., Grace, J., 2007. The human footprint in the carbon cycle of temperate and boreal forests. Nature 447, 849–851. http://dx.doi.org/10.1038/nature05847.

Martin-Benito, D., Kint, V., Del Rio, M., Muys, B., Cañellas, I., 2011. Growth responses of West-Mediterranean Pinus nigra to climate change are modulated by competition and productivity: past trends and future perspectives. For. Ecol. Manage. 262, 1030–1040. http://dx.doi.org/10.1016/j.foreco.2011.05.038.

Matyssek, R., Wieser, G., Ceulemans, R., Rennenberg, H., Pretzsch, H., Haberer, K., Löw, M., Nunn, A.J., Werner, H., Wipfler, P., Oßwald, K., Nikolova, P., Hanke, D.E., Kraigher, H., Tausz, M., Bahnweg, G., Kitao, M., Dieler, J., Sandermann, H., Herbinger, K., Grebenc, T., Blumenröther, M., Deckmyn, G., Grams, T.E.E., Heerdt, C., Leuchner, M., Fabian, P., Häberle, K.-H., 2010. Enhanced ozone strongly reduces carbon sink strength of adult beech (Fagus sylvatica)—resume from the free-air fumigation study at Kranzberg Forest. Environ. Pollut. 158, 2527–2532. http://dx.doi.org/10.1016/j.envpol.2010.05.009.

Meinshausen, M., Vogel, E., Nauels, A., Lorbacher, K., Meinshausen, N., Etheridge, D., Fraser, P., Montzka, S.A., Rayner, P., Trudinger, C., Krummel, P., Beyerle, U., Cannadell, J.G., Daniel, J.S., Enting, I., Law, R.M., O'Doherty, S., Prinn, R.G., Reimann, S., Rubino, M., Velders, G.J.M., Vollmer, M.K., Weiss, R., 2016. Historical greenhouse gas concentrations. Geosci. Model Dev. Discuss. 2016, 1–122. http://dx.doi.org/10.5194/gmd-2016-169.

Mencuccini, M., Martínez-Vilalta, J., Vanderklein, D., Hamid, H.A., Korakaki, E., Lee, S., Michiels, B., 2005. Size-mediated ageing reduces vigour in trees. Ecol. Lett. 8, 1183–1190. http://dx.doi.org/10.1111/j.1461-0248.2005.00819.x.

Michelot, A., Simard, S., Rathgeber, C., Dufrêne, E., Damesin, C., 2012. Comparing the intra-annual wood formation of three European species (Fagus sylvatica, Quercus petraea and Pinus sylvestris) as related to leaf phenology and non-structural carbohydrate dynamics. Tree Physiol. 32, 1033–1045. http://dx.doi.org/10.1093/treephys/tps052.

Mills, G., Pleijel, H., Braun, S., Büker, P., Bermejo, V., Calvo, E., Danielsson, H., Emberson, L., Fernández, I.G., Grünhage, L., Harmens, H., Hayes, F., Karlsson, P.-E., Simpson, D., 2011. New stomatal flux-based critical levels for ozone effects on vegetation. Atmos. Environ. 45, 5064–5068. http://dx.doi.org/10.1016/j.atmosenv.2011.06.009.

Pérez-de-Lis, G., García-González, I., Rozas, V., Olano, J.M., 2016. Feedbacks between earlywood anatomy and non-structural carbohydrates affect spring phenology and wood production in ring-porous oaks. Biogeosciences 13, 5499–5510. http://dx.doi.org/10.5194/bg-13-5499-2016.

Pérez-de-Lis, G., Olano, J.M., Rozas, V., Rossi, S., Vázquez-Ruiz, R.A., García-González, I., 2017. Environmental conditions and vascular cambium regulate carbon allocation to xylem growth in deciduous oaks. Funct. Ecol. 31, 592–603. http://dx.doi.org/10.1111/1365-2435.12789.

Pan, Y., Birdsey, R.A., Fang, J., Houghton, R., Kauppi, P.E., Kurz, W.A., Phillips, O.L., Shvidenko, A., Lewis, S.L., Canadell, J.G., Ciais, P., Jackson, R.B., Pacala, S.W., McGuire, A.D., Piao, S., Rautiainen, A., Sitch, S., Hayes, D., 2011. A large and persistent carbon sink in the world's forests. Science 333, 988–993. http://dx.doi.org/10.1126/science.1201609.

Peñuelas, J., Canadell, J.G., Ogaya, R., 2011. Increased water-use efficiency during the 20th century did not translate into enhanced tree growth. Glob. Ecol. Biogeogr. 20, 597–608. http://dx.doi.org/10.1111/j.1466-8238.2010.00608.x.

Pinheiro, J., Bates, D., 2000. Mixed-Effects Models in S and S-PLUS. Springer Science & Business Media.

Pinheiro, J., Bates, D., DebRoy, S., Sarkar, D., R Core Team, 2016. {nlme}: Linear and Nonlinear Mixed Effects Models} R package version 3. 1–128.

Piovesan, G., Biondi, F., Filippo, A.D., Alessandrini, A., Maugeri, M., 2008. Drought-driven growth reduction in old beech (Fagus sylvatica L.) forests of the central Apennines, Italy. Glob. Change Biol. 14, 1265–1281. http://dx.doi.org/10.1111/j.1365-2486.2008.01570.x.

Pretzsch, H., Dieler, J., Matyssek, R., Wipfler, P., 2010. Tree and stand growth of mature Norway spruce and European beech under long-term ozone fumigation. Environ. Pollut., Facing the Future: Evidence from Joint AspenFACE, SoyFACE and SFB 607 Meeting 158 1061–1070. http://dx.doi.org/10.1016/j.envpol.2009.07.035.

Pretzsch, H., Biber, P., Schütze, G., Uhl, E., Rötzer, T., 2014. Forest stand growth dynamics in Central Europe have accelerated since 1870. Nat. Commun. 5, 4967. http://dx.doi.org/10.1038/ncomms5967.

R Development Core Teame, 2016. R: A language and environment for statistical computing. R Foundation for Statistical Computing, Vienna, Austria.

Rötzer, T., Häberle, K.-H., Kallenbach, C., Matyssek, R., Schütze, G., Pretzsch, H., 2017. Tree species and size drive water consumption of beech/spruce forests—a simulation study highlighting growth under water limitation. Plant Soil 1–20. http://dx.doi.org/

10.1007/s11104-017-3306-x.

Reyer, C., Lasch-Born, P., Suckow, F., Gutsch, M., Murawski, A., Pilz, T., 2013. Projections of regional changes in forest net primary productivity for different tree species in Europe driven by climate change and carbon dioxide. Ann. For. Sci. 71, 211–225. http://dx.doi.org/10.1007/s13595-013-0306-8.

Richardson, A.D., Carbone, M.S., Keenan, T.F., Czimczik, C.I., Hollinger, D.Y., Murakami, P., Schaberg, P.G., Xu, X., 2013. Seasonal dynamics and age of stemwood non-structural carbohydrates in temperate forest trees. New Phytol. 197, 850–861. http://dx.doi.org/10.1111/nph.12042.

Rinn, F., 2003. TSAP-Win. Time series analysis and presentation for dendrochronology and related applications. RINNTECH, Heidelberg.

Scharnweber, T., Manthey, M., Criegee, C., Bauwe, A., Schröder, C., Wilmking, M., 2011. Drought matters − Declining precipitation influences growth of Fagus sylvatica L. and Quercus robur L. in north-eastern Germany. For. Ecol. Manage. 262, 947–961. http://dx.doi.org/10.1016/j.foreco.2011.05.026.

Skomarkova, M.V., Vaganov, E.A., Mund, M., Knohl, A., Linke, P., Boerner, A., Schulze, E.-D., 2006. Inter-annual and seasonal variability of radial growth, wood density and carbon isotope ratios in tree rings of beech (Fagus sylvatica) growing in Germany and Italy. Trees 20, 571–586. http://dx.doi.org/10.1007/s00468-006-0072-4.

Tegel, W., Seim, A., Hakelberg, D., Hoffmann, S., Panev, M., Westphal, T., Büntgen, U., 2014. A recent growth increase of European beech (Fagus sylvatica L.) at its Mediterranean distribution limit contradicts drought stress. Eur. J. For. Res. 133, 61–71. http://dx.doi.org/10.1007/s10342-013-0737-7.

Thomas, F.M., Blank, R., Hartmann, G., 2002. Abiotic and biotic factors and their interactions as causes of oak decline in Central Europe. For. Pathol. 32, 277–307. http://dx.doi.org/10.1046/j.1439-0329.2002.00291.x.

Thornthwaite, C.W., 1948. An approach toward a rational classification of climate. Geogr. Rev. 38, 55–94. http://dx.doi.org/10.2307/210739.

Tricot, C., Vandiepenbeeck, M., Van de Vyver, H., Debontridder, L., 2015. De evolutie van het klimaat in België in Oog voor het klimaat. Koninklijk Meteorologisch Instituut van België, Brussel.

van der Maaten, E., 2012. Climate sensitivity of radial growth in European beech (Fagus sylvatica L.) at different aspects in southwestern Germany. Trees 26, 777–788. http://dx.doi.org/10.1007/s00468-011-0645-8.

Van den Bulcke, J., Wernersson, E.L.G., Dierick, M., Van Loo, D., Masschaele, B., Brabant, L., Boone, M.N., Van Hoorebeke, L., Haneca, K., Brun, A., Luengo Hendriks, C.L., Van Acker, J., 2014. 3D tree-ring analysis using helical X-ray tomography. Dendrochronologia 32, 39–46. http://dx.doi.org/10.1016/j.dendro.2013.07.001.

Vannoppen, A., Maes, S., Kint, V., De Mil, T., Ponette, Q., Van Acker, J., Van den Bulcke, J., Verheyen, K., Muys, B., 2017. Using X-ray CT based tree-ring width data for tree growth trend analysis. Dendrochronologia 44, 66–75. http://dx.doi.org/10.1016/j.dendro.2017.03.003.

Vansteenkiste, D., Van Acker, J., Stevens, M., Le Thiec, D., Nepveu, G., 2007. Composition, distribution and supposed origin of mineral inclusions in sessile oak wood—consequences for microdensitometrical analysis. Ann. For. Sci. 64, 11–19. http://dx.doi.org/10.1051/forest:2006083.

Vieno, M., Heal, M.R., Hallsworth, S., Famulari, D., Doherty, R.M., Dore, A.J., Tang, Y.S., Braban, C.F., Leaver, D., Sutton, M.A., Reis, S., 2014. The role of long-range transport and domestic emissions in determining atmospheric secondary inorganic particle concentrations across the UK. Atmos. Chem. Phys. 14, 8435–8447. http://dx.doi.org/10.5194/acp-14-8435-2014.

Wykoff, W.R., 1990. A basal area increment model for individual conifers in the Northern Rocky Mountains. For. Sci. 36, 1077–1104.

Zeller, L., Ammer, C., Annighöfer, P., Biber, P., Marshall, J., Schütze, G., del Río Gaztelurrutia, M., Pretzsch, H., 2017. Tree ring wood density of Scots pine and European beech lower in mixed-species stands compared with monocultures. For. Ecol. Manage. 400, 363–374. http://dx.doi.org/10.1016/j.foreco.2017.06.018.

Zuur, A.F., Ieno, E.N., Walker, N., Saveliev, A.A., Smith, G.M., 2009. Mixed effects models and extensions in ecology with R, Statistics for Biology and Health. Springer, New York, New York, NY.